Electronic Supplementary Material (ESI) for Physical Chemistry Chemical Physics

Photophysics of Cytosine Tautomers: New Insights into the Nonradiative Decay Mechanisms from MS-CASPT2 Potential Energy Calculations and Excited-State Molecular Dynamics Simulations

Akira Nakayama*, Yu Harabuchi, Shohei Yamazaki†, and Tetsuya Taketsugu

Department of Chemistry, Faculty of Science, Hokkaido University
Sapporo 060-0810, Japan

Electronic Supplementary Information

*To whom correspondence should be addressed. Electronic mail: akira-n@sci.hokudai.ac.jp

†Present address: Department of Frontier Materials Chemistry, Graduate School of Science and Technology, Hirosaki University, Hirosaki 036-8561, Japan

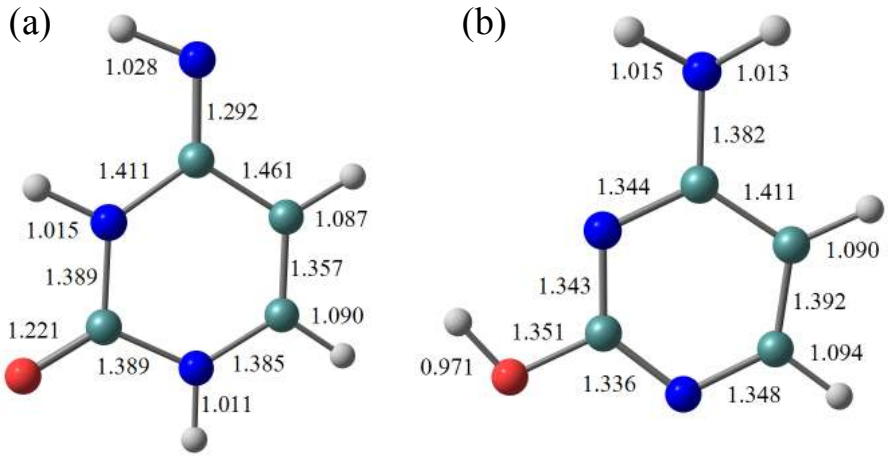

Figure S1. Equilibrium structure in the S_0 state for higher-energy rotamers of (a) imino and (b) enol tautomers. The energies of the imino and enol forms are 0.097 and −0.045 eV relative to the keto form, respectively. The bond lengths are given in units of Å.

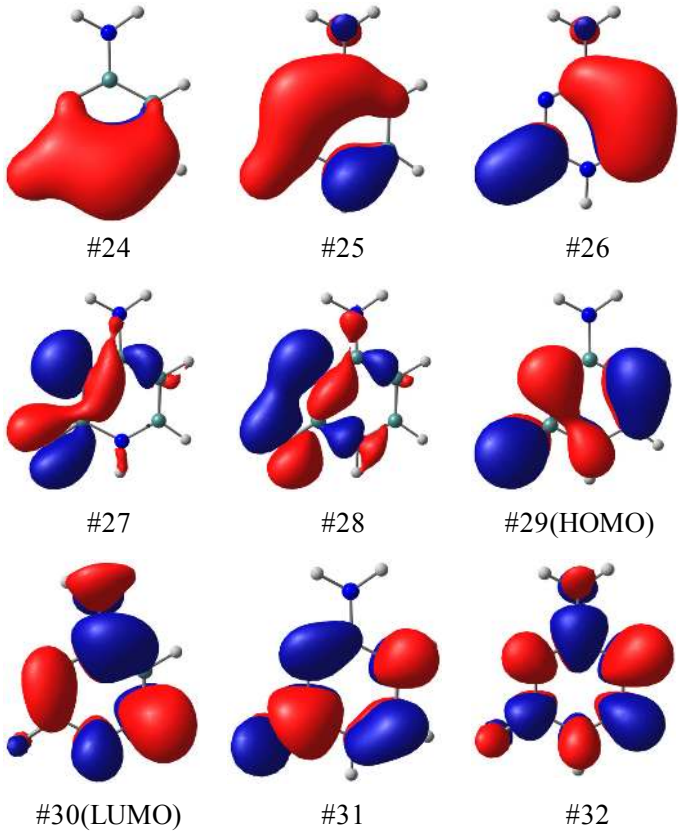

Figure S2. Active orbitals of keto cytosine at $(S_0)_{min}$ in the SA(4)-CASSCF(12,9) calculation.

S_1 minimum energy structure of keto cytosine

When we perform the geometry optimization of keto cytosine in the S_1 state at the SA(2)-CASSCF(12,9) level starting from $(S_0)_{min}$, it is found that the S_1 minimum energy structure is characterized by $^1n_O\pi^*$. It involves the bond inversion of the ring and the elongation of the C2-O7 bond length from 1.222 to 1.362 Å, and also the H1 atom is displaced from the molecular plane. Hereafter this structure is denoted by $(^1n_O\pi^*)'_{min}$ and its structure is given in Figure S3(a). The prime indicates that the structure is optimized by the SA-CASSCF method. The geometry optimization in the $^1\pi\pi^*$ state is also carried out by SA(2)-CASSCF(8,7), where the active space is comprised of only π orbitals. The π orbital that is localized on the N8 atom is excluded from the active space. The optimized geometry is shown in Figure S3(b) and denoted by $(^1\pi\pi^*)'_{min}$. In contrast to $(^1n_O\pi^*)'_{min}$, planarity of the molecule is maintained. The geometrical change from the $(S_0)_{min}$ structure involves the bond inversion of the ring and also the elongation of C2-O7 bond length from 1.222 to 1.327 Å.

The SA(4)-CASSCF(12,9) energy of the S_1 state is 3.64 and 3.81 eV at $(^1n_O\pi^*)'_{min}$ and $(^1\pi\pi^*)'_{min}$, respectively, suggesting that the former exhibits the S_1 global minimum at the SA-CASSCF level. However, the MS(4)-CASPT2(12,9) calculation at the same structures predicts that the S_1 energies at $(^1n_O\pi^*)'_{min}$ and $(^1\pi\pi^*)'_{min}$ relative to $(S_0)_{min}$ are 4.22 and 4.10 eV, respectively, and it is found that $(^1\pi\pi^*)'_{min}$ lies lower than $(^1n_O\pi^*)'_{min}$ at the MS-CASPT2 level.

The optimized structure at the MS(2)-CASPT2(8,7) level is shown in Figure 3(a) in the main document and denoted by $(^1\pi\pi^*)_{min}$. The notable differences between $(^1\pi\pi^*)_{min}$ and $(^1\pi\pi^*)'_{min}$ are the bond lengths of N1-C2, C2-N3, and C2-O7. The MS(4)-CASPT2(12,9) energy at $(^1\pi\pi^*)_{min}$ is calculated to be 3.98 eV relative to $(S_0)_{min}$. We also tried to locate the minimum energy structure in the $^1n_O\pi^*$ state at the MS(3)-CASPT2(6,5) level, starting from the $(^1n_O\pi^*)'_{min}$ structure. The active space is comprised of the four π orbitals (two occupied and two unoccupied) and one lone-pair orbital. The S_1 state at $(^1n_O\pi^*)'_{min}$ is characterized by the $^1n_O\pi^*$ state at MS(3)-CASPT2(6,5) level, but the geometry optimization in the S_1 state leads to the close proximity to $(^1\pi\pi^*)_{min}$ and the S_1 state becomes the $^1\pi\pi^*$ state. Therefore we conclude that the S_1 minimum is characterized by the $^1\pi\pi^*$ state at the MS-CASPT2 level.

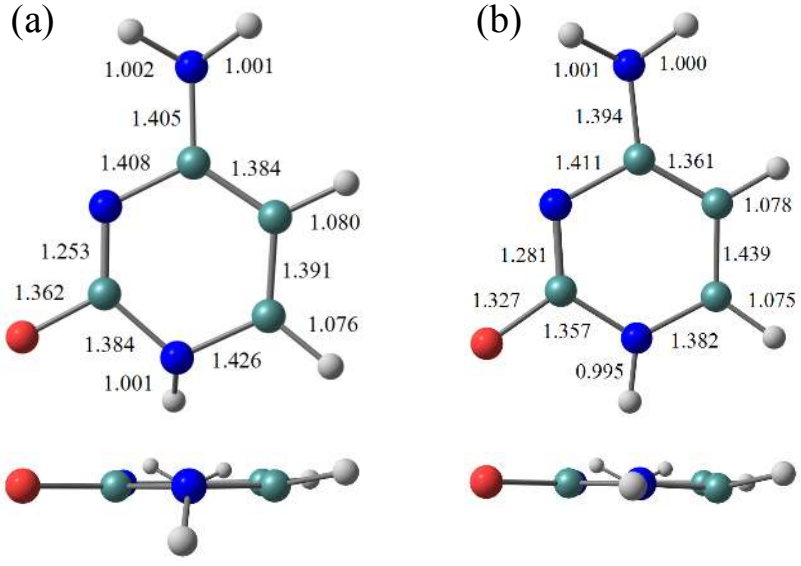

Figure S3. Minimum energy structures of keto cytosine (a) in the $^1n_O\pi^*$ state determined by SA(2)-CASSCF(12,9) method, $(^1n_O\pi^*)'_{min}$, and (b) in the $^1\pi\pi^*$ state determined by SA(2)-CASSCF(8,7) method, $(^1\pi\pi^*)'_{min}$. The bond lengths are given in units of Å.

MEP from $(S_0)_{min}$ for keto cytosine

The MEP computation of keto cytosine in the $^1\pi\pi^*$ state from $(S_0)_{min}$ was performed at the MS(2)-CASPT2(8,7) level of theory with a stepsize of 0.05 bohr·amu$^{1/2}$ and the energetics are reproduced at the MS(4)-CASPT2(12,9) level at selected points along MEP. The MEP calculation was terminated when the plateau region was observed, which was at 1.0 bohr·amu$^{1/2}$ in this case.

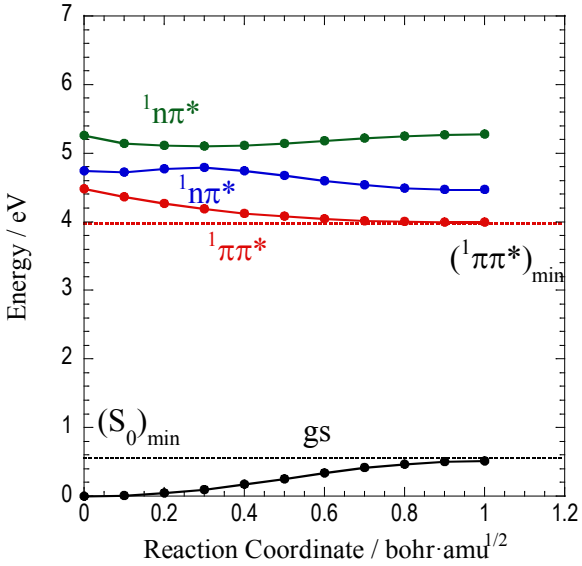

Figure S4. Potential energy profiles of keto cytosine from $(S_0)_{min}$ along the MEP coordinates at the MS(4)-CASPT2(12,9) level. The horizontal dotted lines represent the potential energies of the ground and $^1\pi\pi^*$ states at $(^1\pi\pi^*)_{min}$.

Potential energy profiles from $(S_0)_{min}$ to $(^1n_O\pi^*)'_{min}$

The MS(4)-CASPT2(12,9) potential energy profiles from $(S_0)_{min}$ to $(^1n_O\pi^*)'_{min}$ along LIIC are shown in Figure S5. Clearly it exhibits a minimum before accessing to $(^1n_O\pi^*)'_{min}$ and the electronic structure around this minimum is characterized by the $^1\pi\pi^*$ state. After passing through this minimum, the $^1\pi\pi^*$ and $^1n\pi^*$ states start to mix and then it reaches to $(^1n_O\pi^*)'_{min}$. This behavior is expected since the C2-O7 bond length at $(^1n_O\pi^*)'_{min}$ is longer than that at $(^1\pi\pi^*)_{min}$, and also it involves the out-of-plane displacement of the H1 atom in order to reach $(^1n_O\pi^*)'_{min}$. From these results, it is expected that after photoexcitation to the $^1\pi\pi^*$ state, the molecule will relax toward $(^1\pi\pi^*)_{min}$. It is also seen that the electronic characters of the two $^1n\pi^*$ states (S_2 and S_3) are interchanged along this LIIC points, indicating that the first $^1n\pi^*$ state is rather characterized by the $^1n_N\pi^*$ state at $(S_0)_{min}$.

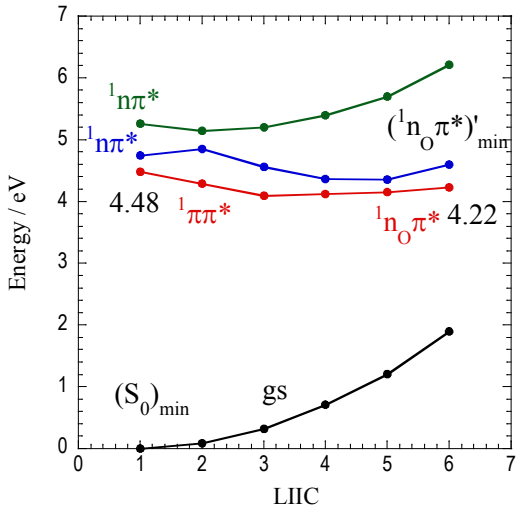

Figure S5. Potential energy profiles for low-lying electronic states of keto cytosine from $(S_0)_{min}$ to $(^1n_O\pi^*)'_{min}$ using LIIC points at the MS(4)-CASPT2(12,9) level.

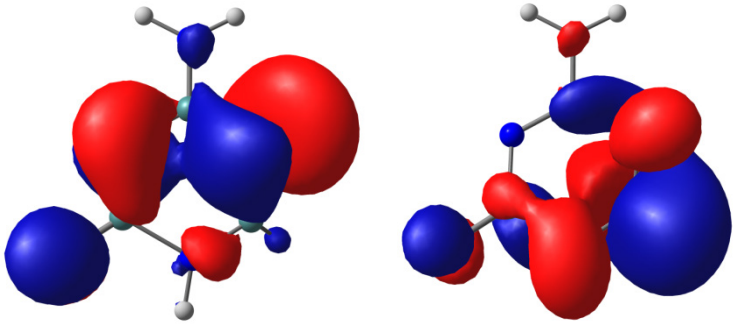

#29(HOMO) #30(LUMO)

Figure S6. SA(2)-CASSCF(8,7) natural orbitals at $(^1\pi\pi^*/gs)_{CI}$ of keto cytosine that are relevant to the excitation.

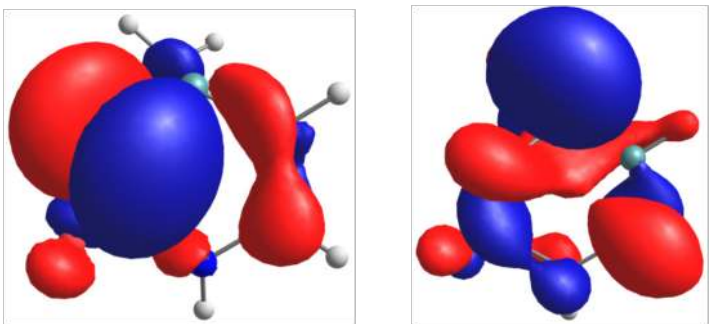

#29(HOMO) #30(LUMO)

Figure S7. SA(2)-CASSCF(8,7) natural orbitals at $(^1\pi_{N3}\pi^*/gs)_{CI}$ of keto cytosine that are relevant to the excitation.

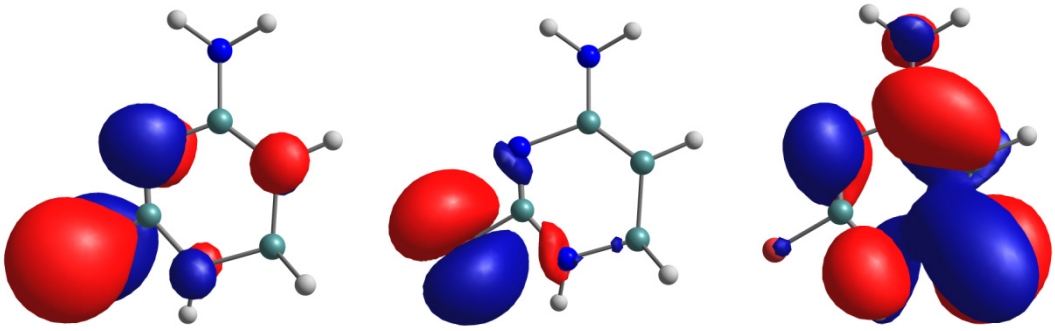

#28(HOMO−1) #29(HOMO) #30(LUMO)

Figure S8. SA(3)-CASSCF(6,5) natural orbitals at $(^1n_O\pi^*/gs)_{CI}$ of keto cytosine that are relevant to the excitation.

Table SI. Configuration Interaction Coefficients for S_0, S_1, and S_2 States in SA(4)-CASSCF(12,9) Calculation at $(^1n_O\pi^*/gs)_{CI}$. CS Stands for Closed Shell Configuration.

	S_0	S_1	S_2
CS	0.053	−0.069	0.682
$^1\pi\pi^*$	−0.660	0.619	0.043
$^1n_O\pi^*$	0.627	0.669	0.015

Table SII. Eigenvectors of the Effective Hamiltonican Matrix in MS(4)-CASPT2(12,9) Calculation at $(^1n_O\pi^*/gs)_{CI}$.

	S_0 (MS-CASPT2)	S_1 (MS-CASPT2)	S_2 (MS-CASPT2)
S_0 (SS-CASPT2)	0.951	−0.215	0.222
S_1 (SS-CASPT2)	−0.308	−0.613	0.727
S_2 (SS-CASPT2)	0.020	0.760	0.650
S_3 (SS-CASPT2)	−0.000	−0.013	−0.013

Potential energy profiles from $(^1\pi\pi^*)_{min}$ to $(^1\pi\pi^*/gs)'_{CI}$ at the different levels of theory

Potential energy profiles from $(^1\pi\pi^*)_{min}$ to $(^1\pi\pi^*/gs)'_{CI}$ are calculated by the SA(4)-CASSCF(12,9), SS-CASPT2(12,9), and MS(4)-CASPT2(12,9) methods, where the MECI point $(^1\pi\pi^*/gs)'_{CI}$ is determined at the SA(2)-CASSCF(8,7) level (see Figures S9 and S10). The potential energies are evaluated at geometries determined by fixing the dihedral angle *d*(N1-C6-C5-H5) at selected values and optimizing the other degrees of freedom in the $^1\pi\pi^*$ state at the SA(2)-CASSCF(8,7) level. Although the SA(4)-CASSCF(12,9) energies of the $^1\pi\pi^*$ and ground states differ by only ~0.2 eV at $d < 90°$, the MS-CASPT2 profile predicts that these two states are separated by more than 1 eV. Also, the MS(4)-CASPT2(12,9) energy of the $^1\pi\pi^*$ state at $(^1\pi\pi^*/gs)'_{CI}$ is calculated to be 4.24 eV, which is higher than that at $(^1\pi\pi^*)'_{min}$ by 0.14 eV. This result is in contrast to the energy profiles given in the main document where $(^1\pi\pi^*/gs)_{CI}$ lies lower than $(^1\pi\pi^*)_{min}$. Another point worth noting is that a crossing of the SS-CASPT2 energies at $d < 90°$ is observed, but it is an artifact since it disappears when the mixing between electronic states are taken into account by MS-CASPT2. These results indicate that the MS-CASPT2 method is more appropriate for both geometry optimization and energetics.

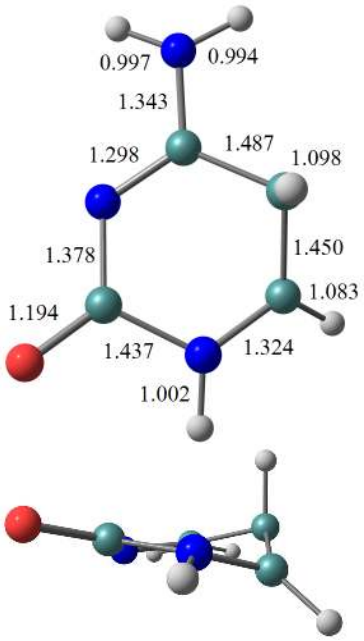

Figure S9. MECI structure $(^1\pi\pi^*/gs)'_{CI}$ of keto cytosine determined by SA(2)-CASSCF(8,7) method. The bond lengths are given in units of Å.

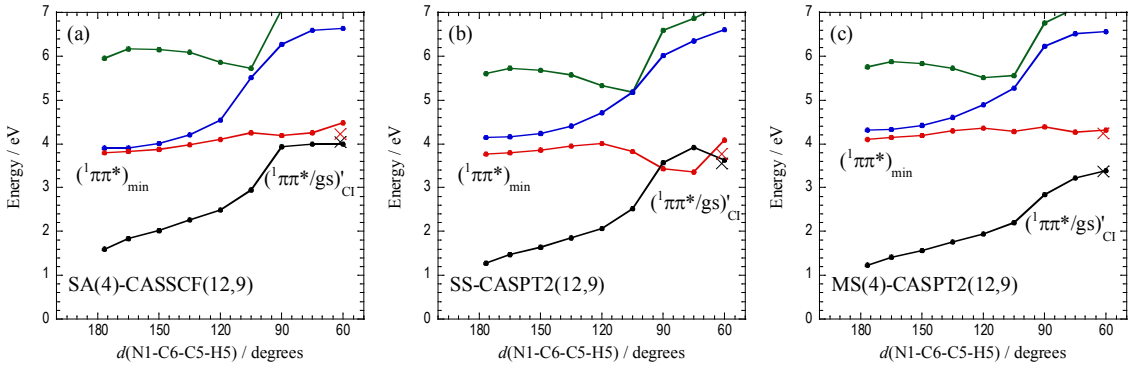

Figure S10. Potential energy profiles for low-lying electronic states of keto cytosine from $(S_0)_{min}$ to $(^1\pi\pi^*/gs)'_{CI}$ at the (a) SA(4)-CASSCF(12,9), (b) SS-CASPT2(12,9), and (c) MS(4)-CASPT2(12,9) levels, as a function of dihedral angle *d*(N1-C6-C5-H5). The potential energies at $(^1\pi\pi^*/gs)'_{CI}$ are shown as cross marks at the respective level.

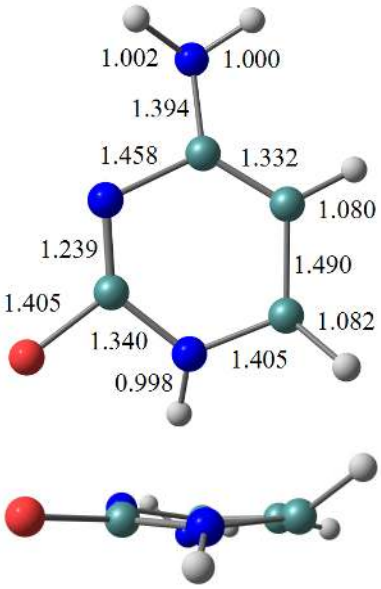

Figure S11. MECI structure $(^1n_O\pi^*/gs)'_{CI}$ of keto cytosine determined by SA(3)-CASSCF(10,8) method. The bond lengths are given in units of Å.

Table SIII Configuration Interaction Coefficients for S_0, S_1, and S_2 States at $(^1n_O\pi^*/gs)'_{CI}$ in SA(4)-CASSCF(12,9) Calculation. CS Stands for Closed Shell Configuration.

	S_0	S_1	S_2
CS	0.120	−0.397	0.671
$^1\pi\pi^*$	0.471	0.718	0.297
$^1n_O\pi^*$	0.777	−0.376	−0.319

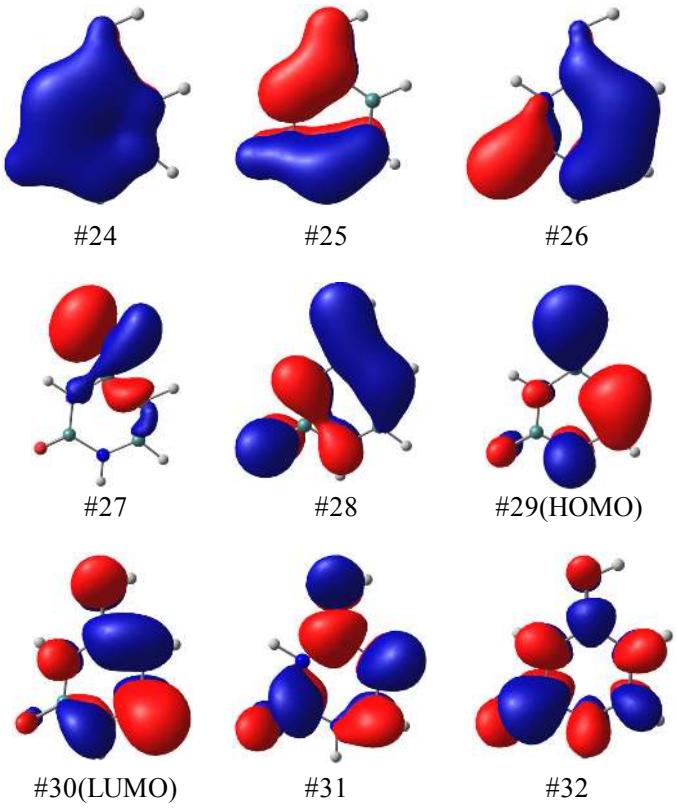

Figure S12. Active orbitals of imino cytosine at $(S_0)_{min}$ in the SA(4)-CASSCF(12,9) calculation.

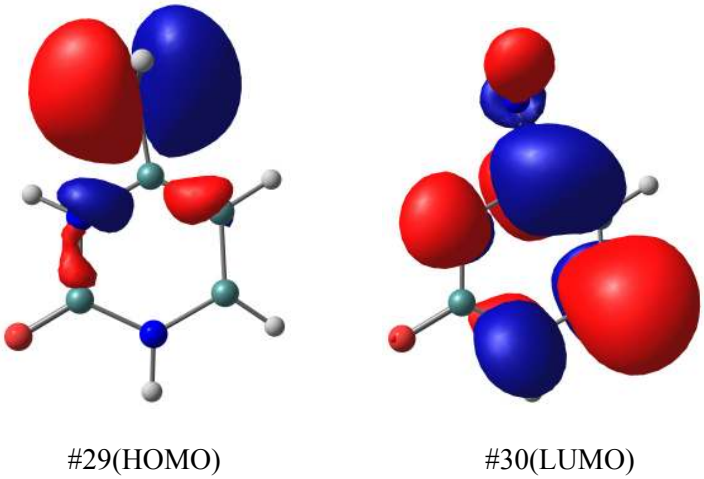

Figure S13. SA(2)-CASSCF(6,5) natural orbitals at $(^1\pi_{N8}\pi^*/gs)_{CI}$ of imino cytosine that are relevant to the excitation.

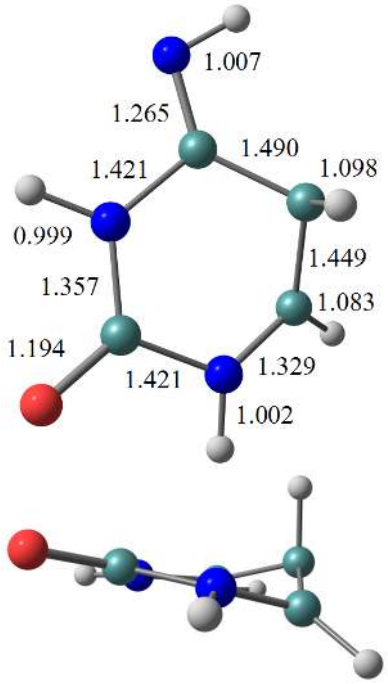

Figure S14. MECI structure $(^{1}\pi\pi^{*}/gs)'_{CI}$ of imino cytosine determined by SA(2)-CASSCF(10,8) method. The bond lengths are given in units of Å.

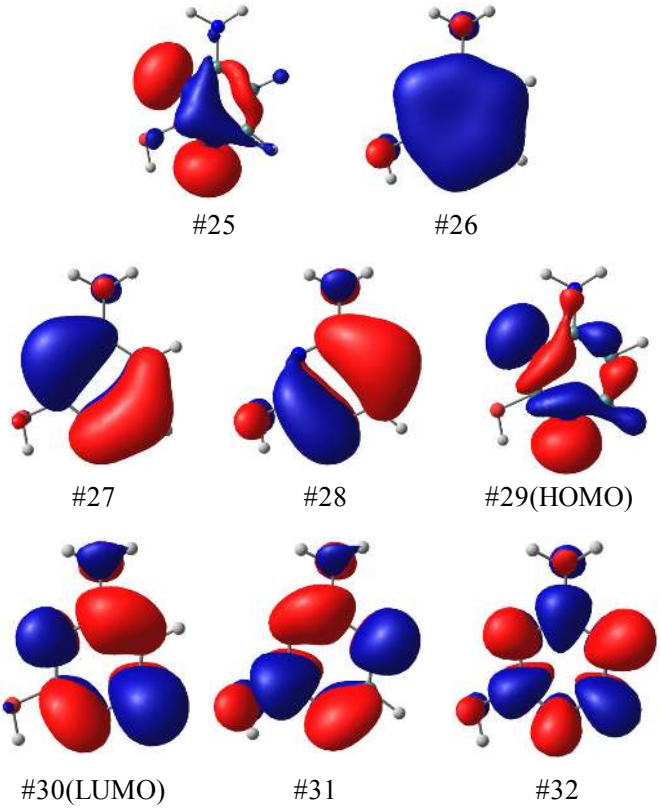

Figure S15. Active orbitals of enol cytosine at $(S_0)_{min}$ in the SA(4)-CASSCF(10,9) calculation.

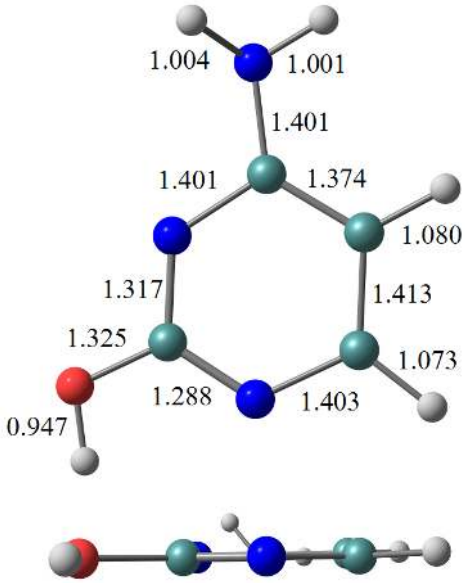

Figure S16. Minimum energy structure of enol cytosine in the $^1n\pi^*$ state determined by SA(4)-CASSCF(10,8) method, $(^1n\pi^*)'_{min}$. The bond lengths are given in units of Å.

MEP from $(S_0)_{min}$ for enol cytosine

The MEP computation of enol cytosine in the $^1\pi\pi^*$ state from $(S_0)_{min}$ was performed at the MS(2)-CASPT2(8,7) level of theory with a stepsize of 0.05 bohr·amu$^{1/2}$ and the energetics are reproduced at the MS(4)-CASPT2(10,8) level at selected points along MEP. The MEP reached a plateau region in the planar structure and thus the calculation was terminated at 1.0 bohr·amu$^{1/2}$. From this structure, the geometry was shifted very slightly toward the direction of the $(^1\pi\pi^*)_{min}$ and the MEP computation was reinitiated. After that, the MEP led to the plateau region again and was terminated at 1.8 bohr·amu$^{1/2}$. It was confirmed that the structure at this point was very close to that at $(^1\pi\pi^*)_{min}$.

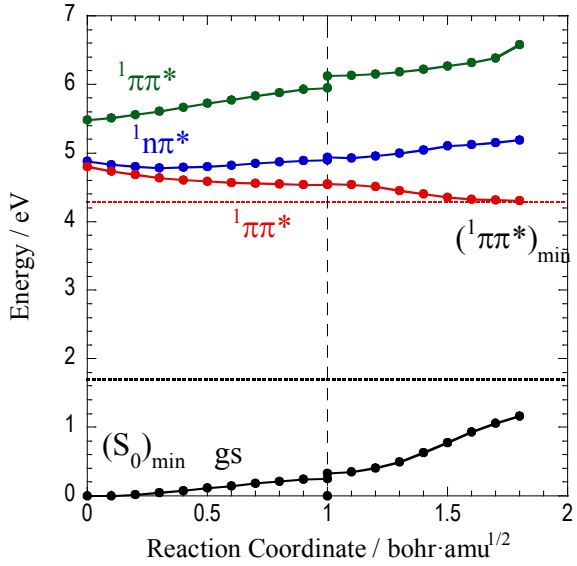

Figure S17. Potential energy profiles of enol cytosine from $(S_0)_{min}$ along the MEP coordinates at the MS(4)-CASPT2(10,8) level. The horizontal dotted lines represent the potential energies of the ground and $^1\pi\pi^*$ states at $(^1\pi\pi^*)_{min}$. The vertical dashed line represents the reaction coordinate at which the MEP was terminated once since it reached a plateau region in the planar structure.

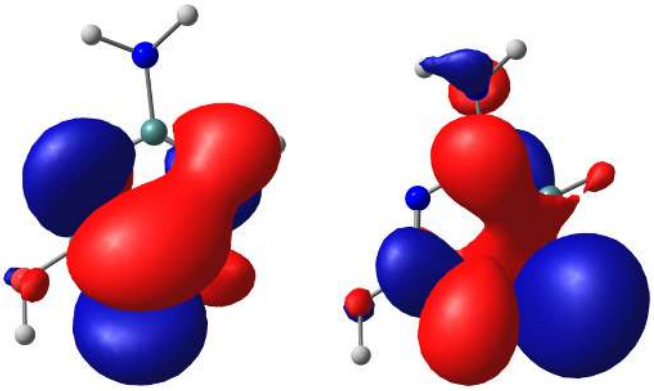

#29(HOMO) #30(LUMO)

Figure S18. SA(2)-CASSCF(8,7) natural orbitals at $(^1\pi_{N1}\pi^*/gs)_{CI}$ of enol cytosine that are relevant to the excitation.

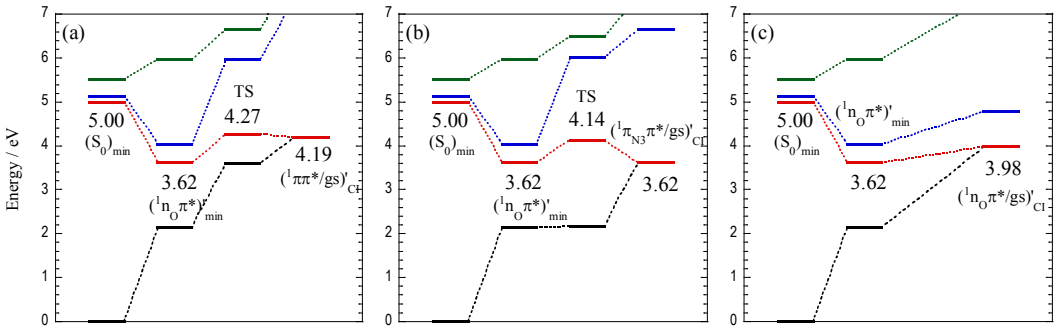

Figure S19. SA(4)-CASSCF(12,9) electronic energies of the $(S_0)_{min}$, $(S_1)_{min}$ = $(^1n_O\pi^*)'_{min}$, TS, and MECI structures for keto cytosine, where the latter three structures are optimized at the SA(4)-CASSCF(12,9) level (indicated by prime). The TS structure is determined by the highest point along the reaction path, which is obtained by excited-state geometry optimizations at fixed values of the same driving coordinate as used in the MS-CASPT2 optimization. For the MECI optimization, the projected gradient method by Bearpark *et al*. (Ref. 69 of the main document) is applied.

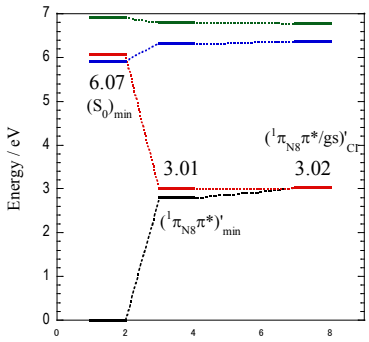

Figure S20. SA(4)-CASSCF(12,9) electronic energies of the $(S_0)_{min}$, $(S_1)_{min}$ = $(^1\pi_{N8}\pi^*)'_{min}$, and $(^1\pi_{N8}\pi^*/gs)_{CI}$ structures for imino cytosine, where the latter two structures are optimized at the SA(4)-CASSCF(12,9) level (indicated by prime).

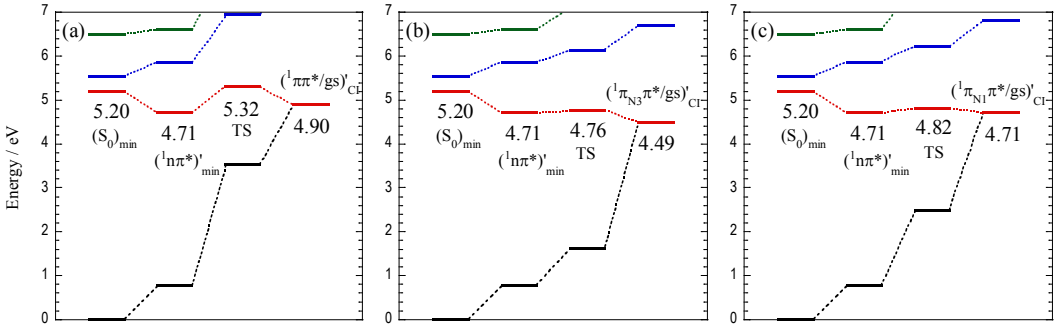

Figure S21. SA(4)-CASSCF(10,8) electronic energies of the $(S_0)_{min}$, $(S_1)_{min}$ = $(^1n\pi^*)'_{min}$, TS, and MECI structures for enol cytosine, where the latter three structures are optimized at the SA(4)-CASSCF(10,9) level (indicated by prime).